Supporting Information

Controllable topological phase transition via ferroelectric-paraelectric switching in ferromagnetic single-layer $M_IM_{II}Ge_2X_6$ family

Jingbo Bai,[1] Tie Yang,[1] Zhenzhou Guo,[3*] Ying Liu,[2] Yalong Jiao,[2] Weizhen Meng,[2*] Zhenxiang Cheng[3*]

1. School of Physical Science and Technology, Southwest University, Chongqing 400715, China.

2. College of Physics, Hebei Key Laboratory of Photophysics Research and Application, Hebei Normal University, Shijiazhuang 050024, China.

3. Institute for Superconducting and Electronic Materials, University of Wollongong, Wollongong, 2500, Australia.

[*]Email: zg855@uowmail.edu.au, mengweizhen@hebtu.edu.cn, cheng@uow.edu.au

Table SI. Wyckoff sites of atoms in ferroelectric (FE) and paraelectric (PE) phases of 11 2D multiferroic materials.

Materials	PE	FE
$ReIrGe_2S_6$	S (*6l*) (0.32983, 0.03906, 0.42971) Ir (*1b*) (0.00000, 0.00000, 0.50000) Re (*1f*) (0.66667, 0.33333, 0.50000) Ge (*2h*) (0.33333, 0.66667, 0.55602)	S1 (*3d*) (0.33108,0.04411,0.45785) S2 (*3d*) (0.98402,0.66965,0.53975) Ir (*1a*) (0.00000,0.00000,0.49884) Re (*1c*) (0.66667,0.33333,0.49755) Ge (*1b*) (0.33333,0.66667,0.515790) Ge (*1b*) (0.33333,0.66667,0.43195)
$ReIrGe_2Se_6$	S (*6l*) (0.32936,0.04187,0.42584) Ir (*1b*) (0.00000,0.00000,0.50000) Re (*1f*) (0.66667,0.33333,0.50000) Ge (*2h*) (0.33333,0.66667,0.55680)	Se1 (*3d*) (0.32997,0.04946,0.45454) Se2 (*3d*) (0.98100,0.66994,0.54285) Ir (*1a*) (0.00000,0.00000,0.49940) Re (*1c*) (0.66667,0.33333,0.49805) Ge (*1b*) (0.33333,0.66667,0.51518) Ge (*1b*) (0.33333,0.66667,0.43213)
$ReAlGe_2Se_6$	Se (*6l*) (0.33813,0.04085,0.42319) Al (*1b*) (0.00000,0.00000,0.50000) Re (*1f*) (0.66667,0.33333,0.50000) Ge (*2h*) (0.33333,0.66667,0.55641)	Se1 (*3d*) (0.33245,0.04762,0.45279) Se2 (*3d*) (0.98008,0.65584,0.54483) Al (*1a*) (0.00000,0.00000,0.50299) Re (*1c*) (0.66667,0.33333,0.49761) Ge (*1b*) (0.33333,0.66667,0.51383) Ge (*1b*) (0.33333,0.66667,0.42964)
$ReBiGe_2Se_6$	S (*6l*) (0.37520,0.03798,0.43527) Bi (*1b*) (0.00000,0.00000,0.50000) Re (*1f*) (0.66667,0.33333,0.50000) Ge (*2h*) (0.33333,0.66667,0.54659)	Se1 (*3d*) (0.37126,0.03889,0.42896) Se2 (*3d*) (0.96119,0.62884,0.55843) Bi (*1a*) (0.00000,0.00000,0.49365) Re (*1c*) (0.66667,0.33333,0.49372) Ge (*1b*) (0.33333,0.66667,0.59437) Ge (*1b*) (0.33333,0.66666,0.39302)
$ReRhGe_2Se_6$	Se (*6l*) (0.32955,0.04165,0.42522) Rh (*1b*) (0.00000,0.00000,0.50000) Re (*1f*) (0.66667,0.33333,0.50000) Ge (*2h*) (0.33333,0.66667,0.55699)	Se1 (*3d*) (0.32950,0.04877,0.45425) Se2 (*3d*) (0.98025,0.66870,0.54304) Rh (*1a*) (0.00000,0.00000,0.49960) Re (*1c*) (0.66667,0.33333,0.49818) Ge (*1b*) (0.33333,0.66667,0.51512) Ge (*1b*) (0.33333,0.66667,0.43215)
$ReSnGe_2S_6$	S (*6l*) (0.36300,0.04025,0.43634) Sn (*1b*) (0.00000,0.00000,0.50000) Re (*1f*) (0.66667,0.33333,0.50000) Ge (*2h*) (0.33333,0.66666,0.54862)	S1 (*3d*) (0.35381,0.05032,0.45815) S2 (*3d*) (0.97866,0.62496,0.53792) Sn (*1a*) (0.00000,0.00000,0.50178) Re (*1c*) (0.66667,0.33333,0.49656) Ge (*1b*) (0.33333,0.66667,0.51280) Ge (*1b*) (0.33333,0.66667,0.43757)
$TcIrGe_2S_6$	S (*6l*) (0.32882,0.03756,0.43995) Ir (*1b*) (0.00000,0.00000,0.50000) Tc (*1f*) (0.66667,0.33333,0.50000) Ge (*2h*) (0.33333,0.66667,0.54705)	S1 (*3d*) (0.33116,0.03889,0.45833) S2 (*3d*) (0.98425,0.67090,0.53951) Ir (*1a*) (0.00000,0.00000,0.49871) Tc (*1c*) (0.66667,0.33333,0.49735) Ge (*1b*) (0.33333,0.66667,0.51617)

		Ge (*1b*) (0.33333,0.66667, 0.43119)
$TcIrGe_2Se_6$	Se (*6l*) (0.32841,0.04052,0.42790) Ir (*1b*) (0.00000,0.00000,0.50000) Tc (*1f*) (0.66667,0.33333,0.50000) Ge (*2h*) (0.33333,0.66667,0.55444)	Se1 (*3d*) (0.32970,0.04649,0.45088) Se2 (*3d*) (0.98113,0.67074,0.54755) Ir (*1a*) (0.00000,0.00000,0.49993) Tc (*1c*) (0.66667,0.33333,0.49834) Ge (*1b*) (0.33333,0.66667,0.51762) Ge (*1b*) (0.33333,0.66667,0.42577)
$WIrGe_2S_6$	S (*6l*) (0.32375,0.03188 ,0.42803) Ir (*1b*) (0.00000,0.00000,0.50000) W (*1f*) (0.66667,0.33333,0.50000) Ge (*2h*) (0.33333,0.66667,0.55453)	S1 (*3d*) (0.32970,0.04649,0.45088) S2 (*3d*) (0.98113,0.67074,0.54755) Ir (*1a*) (0.00000,0.00000,0.49993) W (*1c*) (0.66667,0.33333,0.49834) Ge (*1b*) (0.33333,0.66667,0.51762) Ge (*1b*) (0.33333,0.66667,0.42577)
$WAlGe_2Se_6$	Se (*6l*) (0.33265,0.03360,0.42464) Al (*1b*) (0.00000,0.00000,0.50000) W (*1f*) (0.66667,0.33333,0.50000) Ge (*2h*) (0.33333,0.66667,0.55466)	Se1 (*3d*) (0.34337,0.01809,0.45481) Se2 (*3d*) (0.95702,0.66433,0.54672) Al (*1a*) (0.00000,0.00000,0.49776) W (*1c*) (0.66667,0.33333,0.50068) Ge (*1b*) (0.33333,0.66667,0.57297) Ge (*1b*) (0.33333,0.66667,0.48708)
$WPtGe_2Te_6$	Te (*6l*) (0.32964,0.04144,0.42129) Pt (*1b*) (0.00000,0.00000,0.50000) Re (*1f*) (0.66667,0.33333,0.50000) Ge (*2h*) (0.33333,0.66667,0.55828)	Te1 (*3d*) (0.32956,0.05872,0.44866) Te2 (*3d*) (0.98337,0.67228,0.54713) Pt (*1a*) (0.00000,0.00000,0.49941) W (*1c*) (0.66667,0.33333,0.49818) Ge (*1b*) (0.33333,0.66666,0.51568) Ge (*1b*) (0.33333,0.66667,0.43633)

Table SII. Lattice constants of ferroelectric (FE) and paraelectric (PE) phases for 11 2D multiferroic materials.

Materials	PE	FE
$ReIrGe_2S_6$	a=b=6.11 Å	a=b=6.26 Å
$ReIrGe_2Se_6$	a=b=6.44 Å	a=b=6.57 Å
$ReAlGe_2Se_6$	a=b=6.43 Å	a=b=6.52 Å
$ReBiGe_2Se_6$	a=b=6.37 Å	a=b=6.51 Å
$ReRhGe_2Se_6$	a=b=6.42 Å	a=b=6.55 Å
$ReSnGe_2S_6$	a=b=6.33 Å	a=b=6.45 Å
$TcIrGe_2S_6$	a=b=6.08 Å	a=b=6.23 Å
$TcIrGe_2Se_6$	a=b=6.41 Å	a=b=6.55 Å

$WIrGe_2S_6$	a=b=6.08 Å	a=b=6.29 Å
$WAlGe_2Se_6$	a=b=6.47 Å	a=b=6.55 Å
$WPtGe_2Te_6$	a=b=7.03 Å	a=b=7.09 Å

Table SIII. Ferroelectric transition barriers for the SL $M_IM_{II}Ge_2X_6$ family.

Materials	Energy barrier (eV)	Materials	Energy barrier (eV)
$ReIrGe_2S_6$	0.62	$ReIrGe_2Se_6$	0.23
$TcIrGe_2S_6$	0.49	$ReRhGe_2Se_6$	0.19
$ReAlGe_2Se_6$	0.07	$WPtGe_2Te_6$	0.16
$WIrGe_2S_6$	0.77	$WAlGe_2Se_6$	0.22
$ReSnGe_2Se_6$	0.20	$ReBiGe_2Se_6$	0.24

Table SIV. Magnetic ground states of ferroelectric (FE) phase for 11 2D multiferroic materials.

Materials	FM (eV)	AFM1 (eV)	AFM2 (eV)
$ReIrGe_2S_6$	-226.32145395	-226.14374067	-226.14374197
$ReIrGe_2Se_6$	-222.62311261	-222.15396648	-222.14701290
$ReAlGe_2Se_6$	-204.84004770	-204.45416126	-204.45347128
$ReBiGe_2Se_6$	-204.84004770	-204.45416126	-204.45347128
$ReRhGe_2Se_6$	-195.76309287	-195.51162751	-195.51162879
$ReSnGe_2S_6$	-210.25680034	-210.12374933	-210.12349296
$TcIrGe_2S_6$	-187.83463627	-187.57906846	-187.57906987
$TcIrGe_2Se_6$	-203.81887192	-203.68401305	-203.68445755
$WIrGe_2S_6$	-232.32182864	-232.13392289	-232.13392147
$WAlGe_2Se_6$	-198.86190839	-198.63532164	-198.63591126
$WPtGe_2Te_6$	-205.93188200	-205.54534612	-205.54534552

Table SV. Fractional corner charges of SL-$ReBiGe_2S_6$, SL-$WIrGe_2S_6$, SL-$TcIrGe_2S_6$, SL-$TcIrGe_2Se_6$, and SL-$ReIrGe_2S_6$.

2D multiferroic materials		Spin-up			Spin-down		
		$\#K_{2\uparrow}^{3}$	$\#\Gamma_{2\uparrow}^{3}$	$Q_{c\uparrow}^{(3)}$	$\#K_{2\downarrow}^{3}$	$\#\Gamma_{2\downarrow}^{3}$	$Q_{c\downarrow}^{(3)}$
$ReBiGe_2S_6$	PE	14	15	2e/3	-	-	-
	FE	-	-	-	-	-	-
$WIrGe_2S_6$	PE	-	-	-	12	13	2e/3
	FE	-	-	-	12	13	2e/3
$TcIrGe_2S_6$	PE	13	15	e/3	-	-	-
	FE	13	15	e/3	13	14	2e/3

$TcIrGe_2Se_6$	PE	14	15	2e/3	-	-	-
	FE	14	15	2e/3	12	13	2e/3

$ReIrGe_2S_6$	K_1	K_2	K_1’	K_2’	Q_{conner}
Spin-up	-2	0	-	-	e/3
Spin-dn	-2	0	-	-	e/3

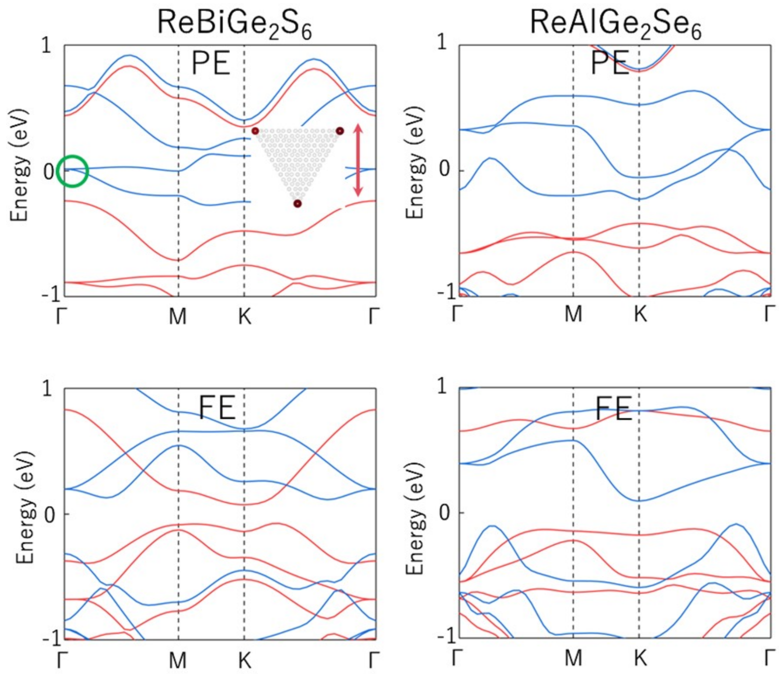

Fig. S 1 Electronic band structures of PE and FE phases for $ReBiGe_2S_6$ and $ReAlGe_2Se_6$.

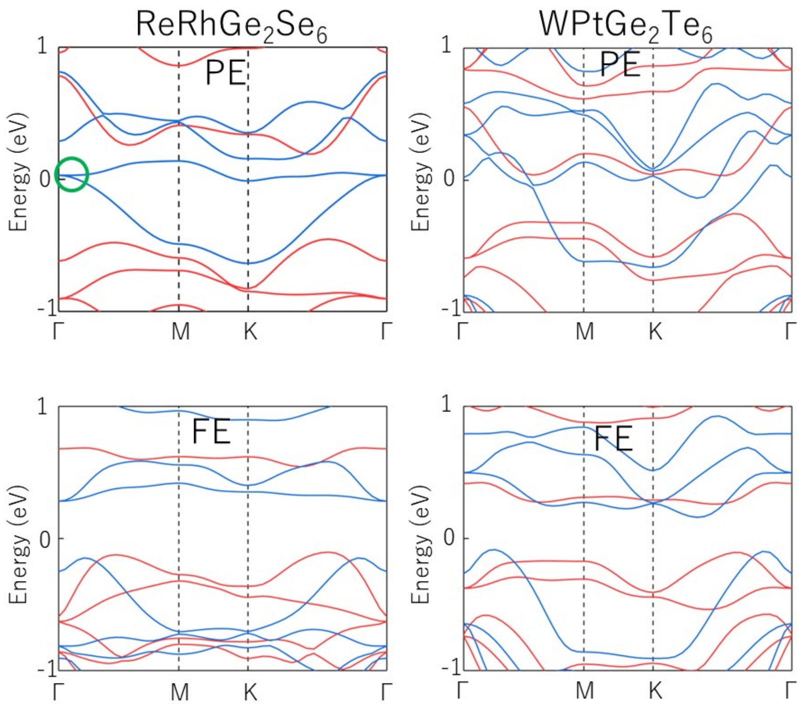

Fig. S 2 Electronic band structures of PE and FE phases for $ReRhGe_2Se_6$ and $WPtGe_2Te_6$.

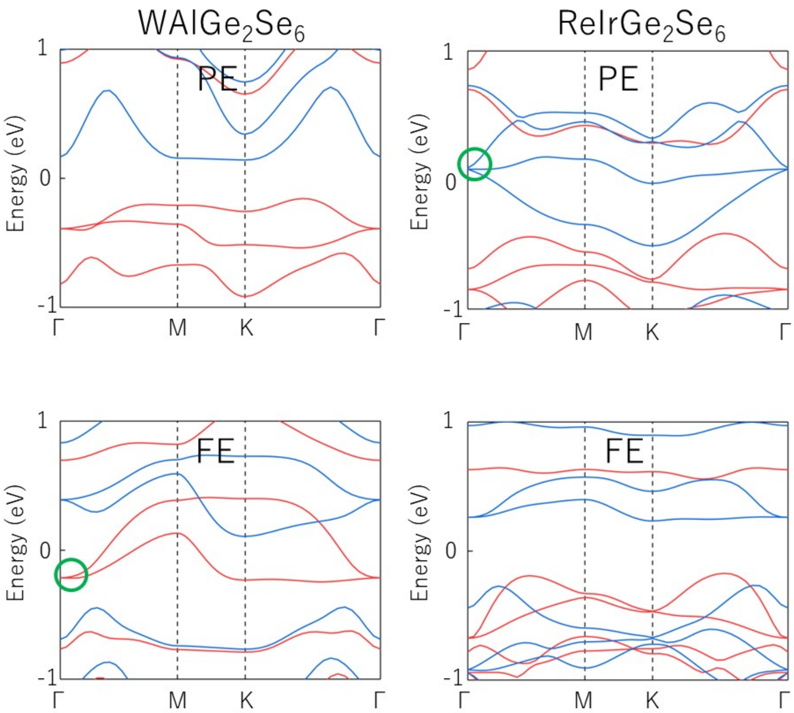

Fig. S 3 Electronic band structures of PE and FE phases for $WAlGe_2Se_6$ and $ReIrGe_2Se_6$.

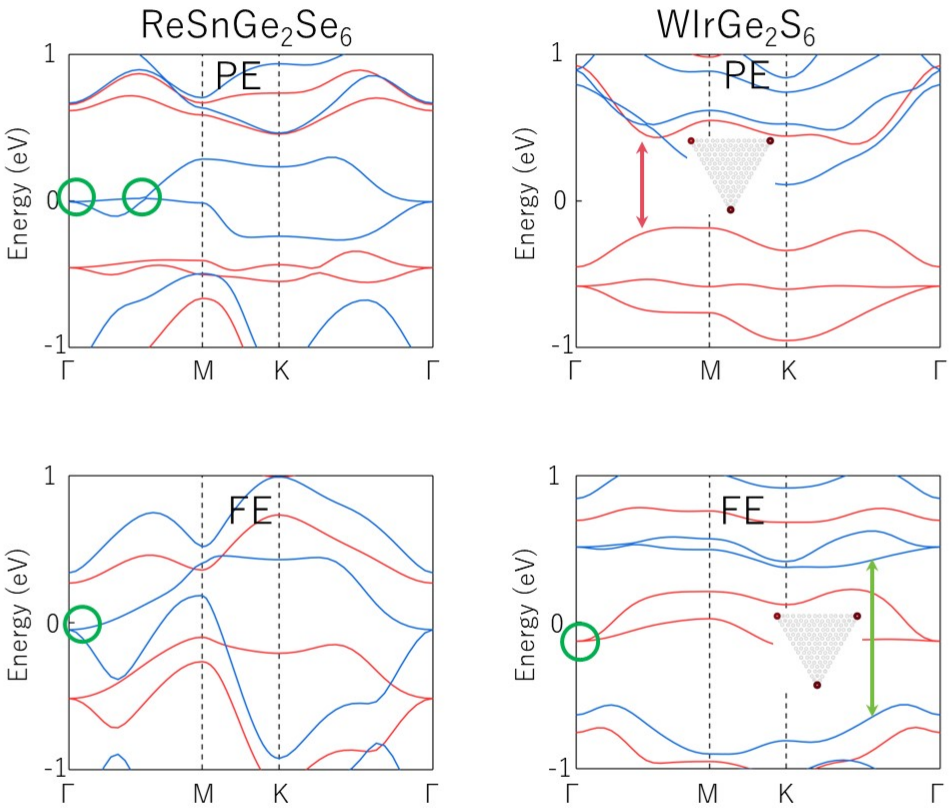

Fig. S 4 Electronic band structures of PE and FE phases for $ReSnGe_2Se_6$ and $WIrGe_2S_6$.

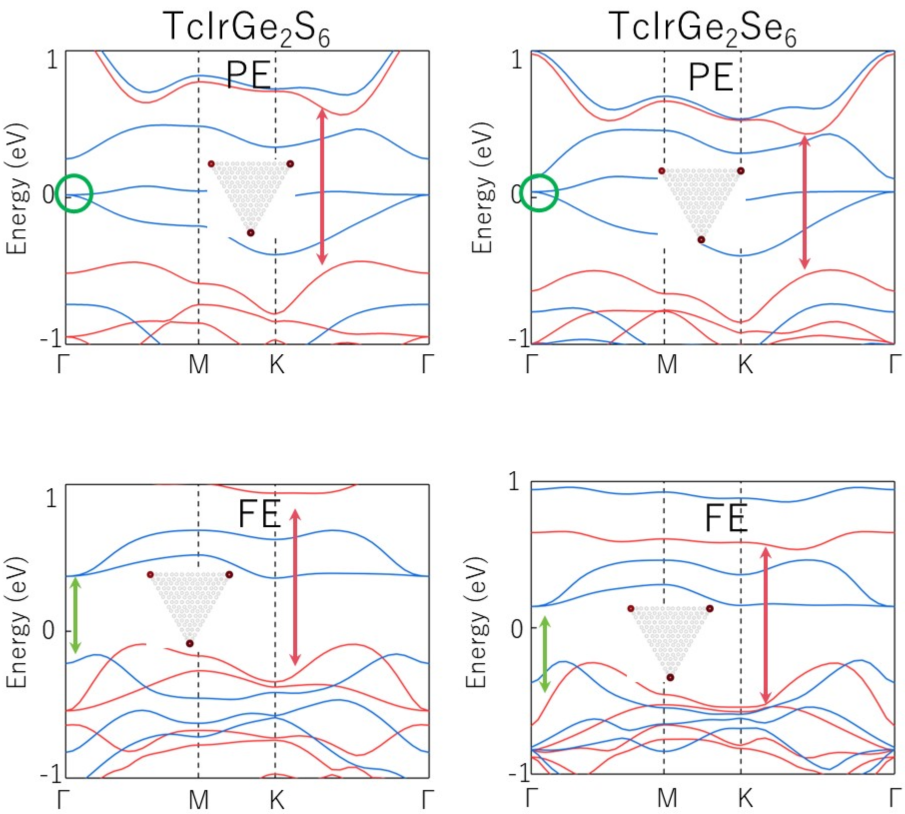

Fig. S 5 Electronic band structures of PE and FE phases for $TcIrGe_2Se_6$ and $TcIrGe_2S_6$.

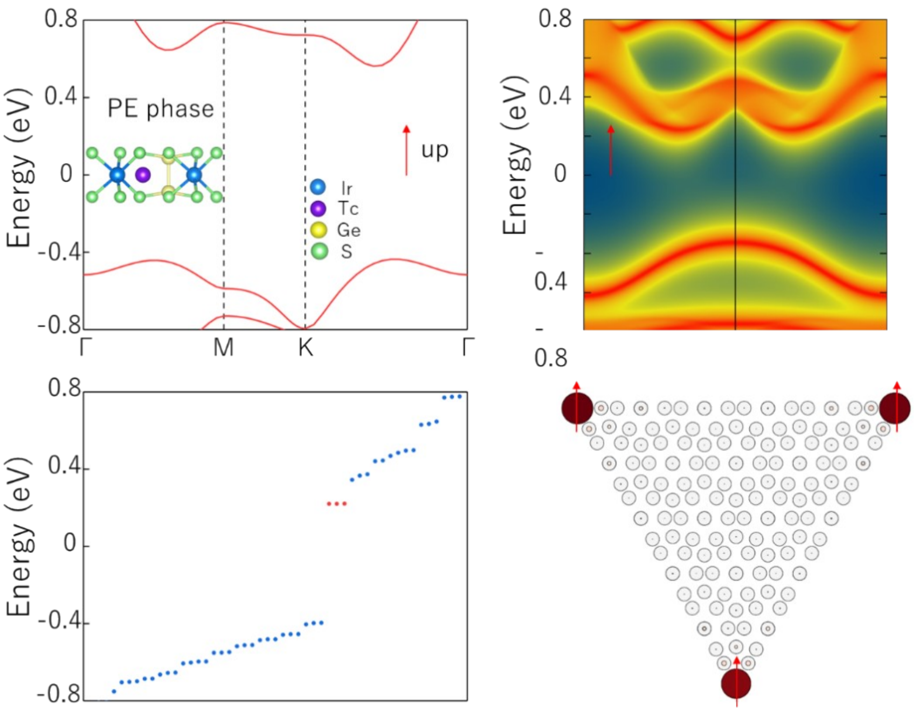

Fig. S 6 (a) Electronic band structures of PE phases in spin-up channel for $TcIrGe_2S_6$. (b) Projected spectrum in spin-up channel for $TcIrGe_2S_6$. (c) The corresponding energy levels in spin-up channel for $TcIrGe_2S_6$. (d) The charge distribution of the finite-sized nanodisks.

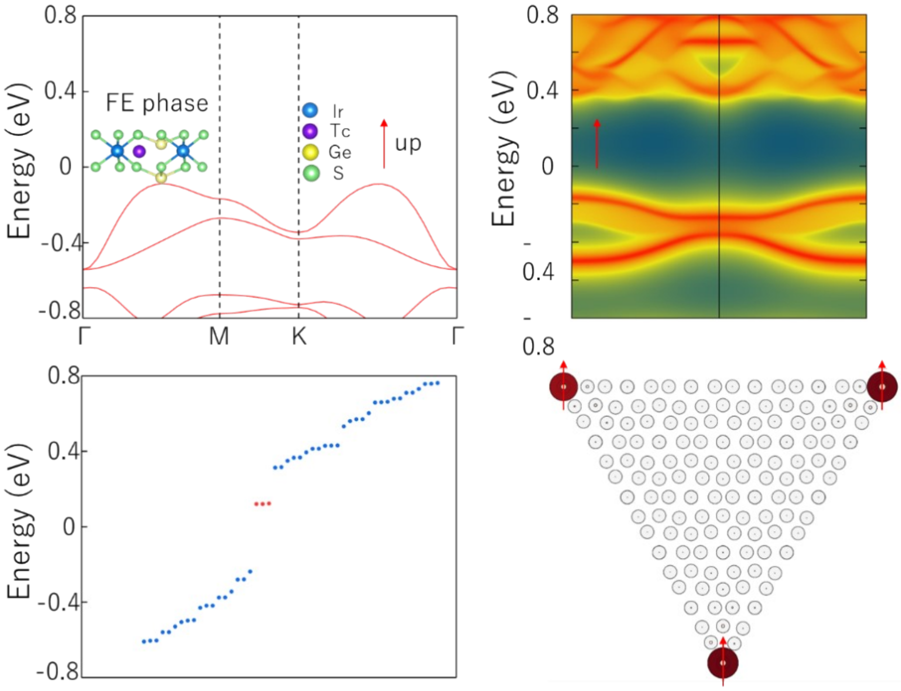

Fig. S 7 (a) Electronic band structures of FE phases in spin-up channel for $TcIrGe_2S_6$. (b) Projected spectrum in spin-up channel for $TcIrGe_2S_6$. (c) The corresponding energy levels in spin-up channel for $TcIrGe_2S_6$. (d) The charge distribution of the finite-sized nanodisks.

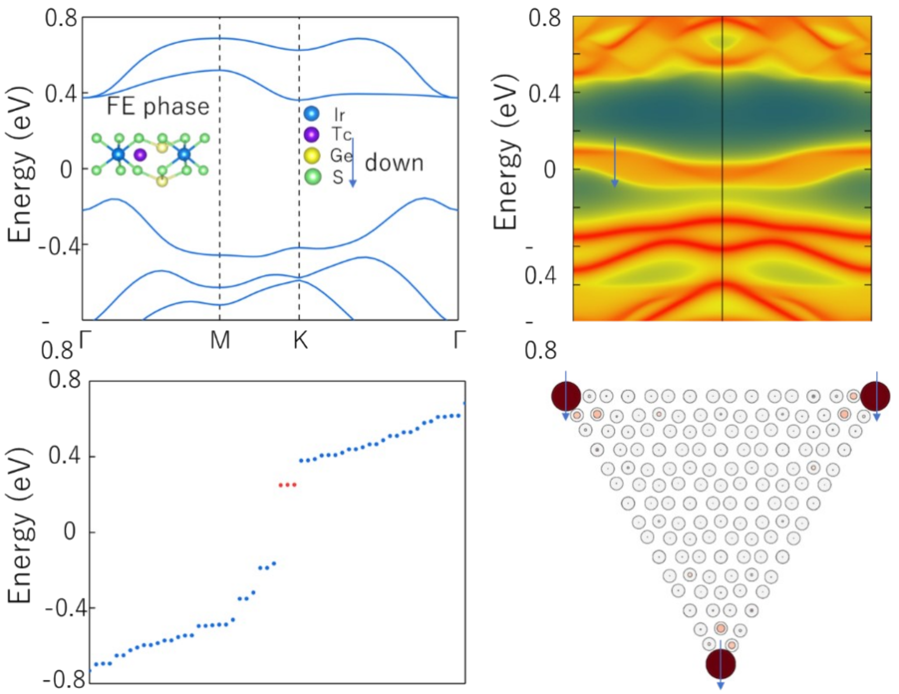

Fig. S 8 (a) Electronic band structures of FE phases in spin-down channel for $TcIrGe_2S_6$. (b) Projected spectrum in spin-down channel for $TcIrGe_2S_6$. (c) The corresponding energy levels in spin-down channel for $TcIrGe_2S_6$. (d) The charge distribution of the finite-sized nanodisks.

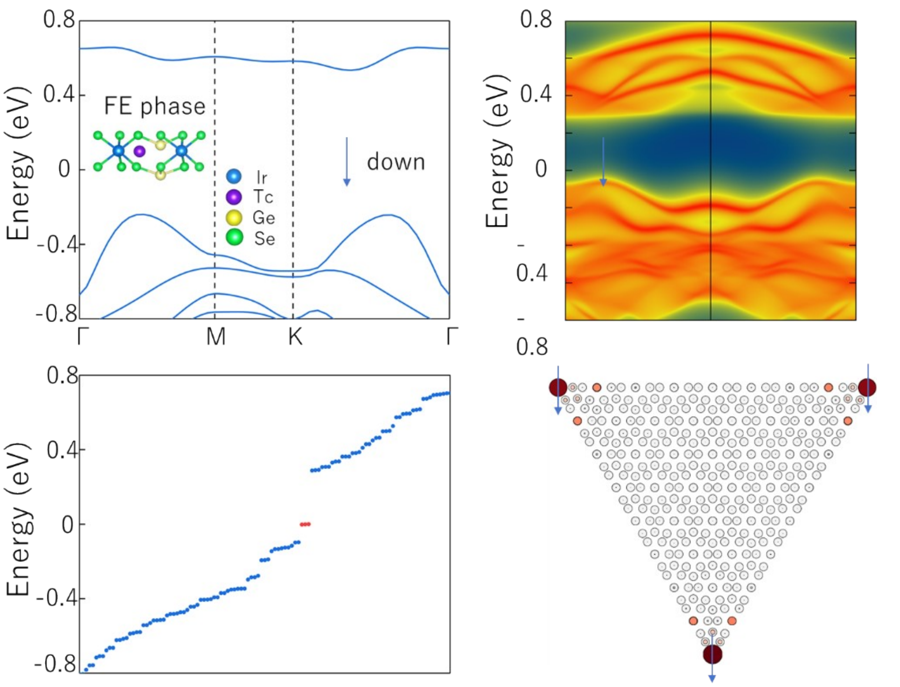

Fig. S 9 (a) Electronic band structures of FE phases in spin-down channel for $TcIrGe_2Se_6$. (b) Projected spectrum in spin-down channel for $TcIrGe_2Se_6$. (c) The corresponding energy levels in spin-down channel for $TcIrGe_2S_6$. (d) The charge distribution of the finite-sized nanodisks.

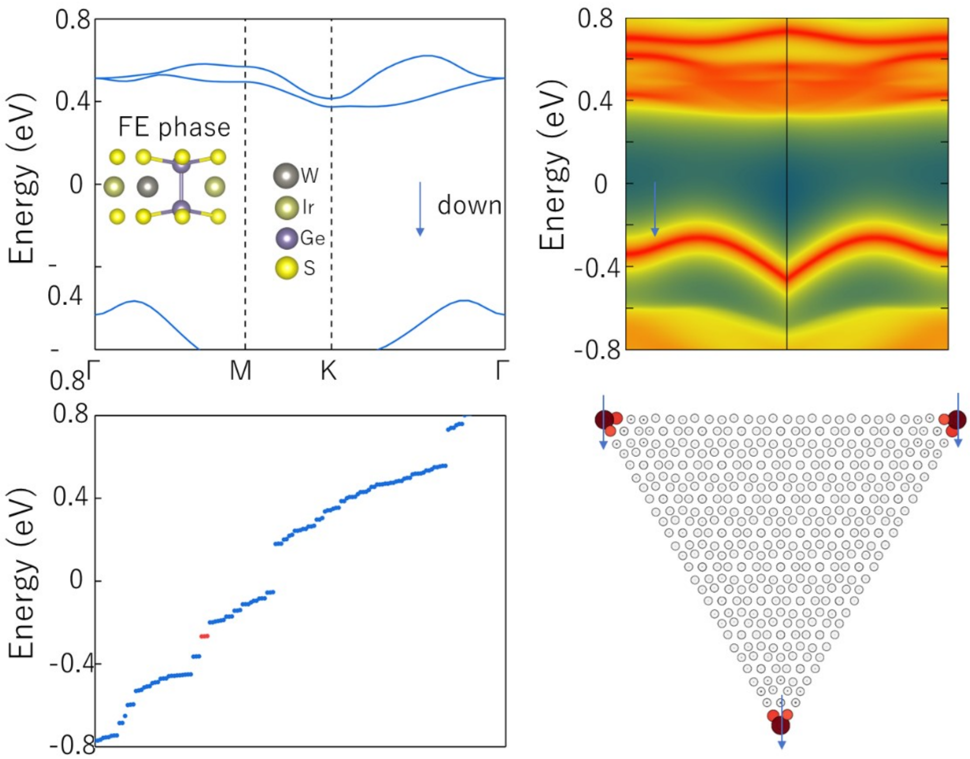

Fig. S 10 (a) Electronic band structures of FE phases in spin-down channel for $WIrGe_2S_6$. (b) Projected spectrum in spin-down channel for $WIrGe_2S_6$. (c) The corresponding energy levels in spin-down channel for $WIrGe_2S_6$. (d) The charge distribution of the finite-sized nanodisks.

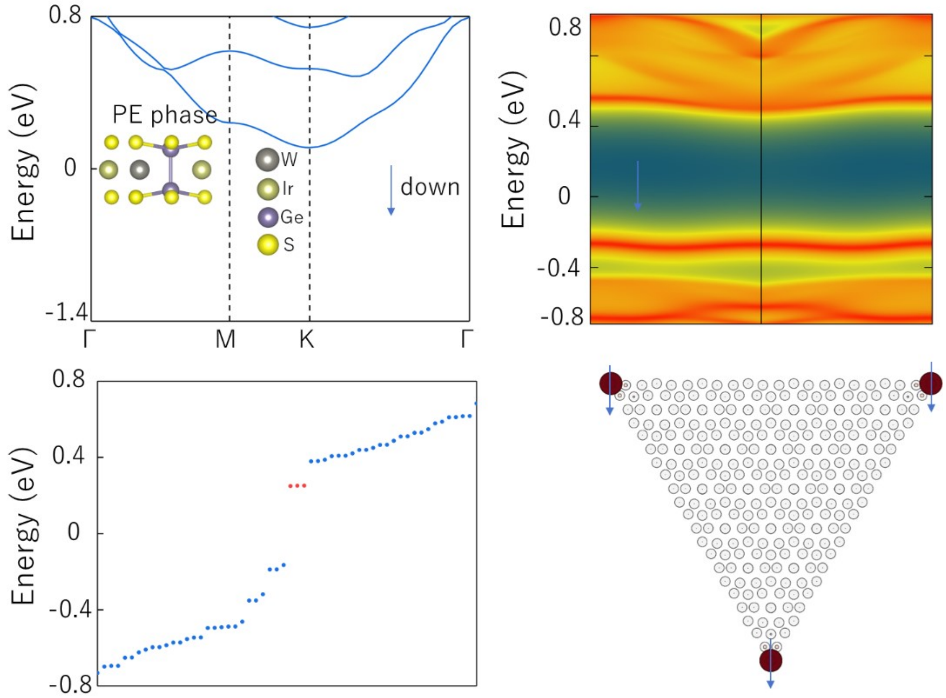

Fig. S 11 (a) Electronic band structures of PE phases in spin-down channel for $WIrGe_2S_6$. (b) Projected spectrum in spin-down channel for $WIrGe_2S_6$. (c) The corresponding energy levels in spin-down channel for $WIrGe_2S_6$. (d) The charge distribution of the finite-sized nanodisks.

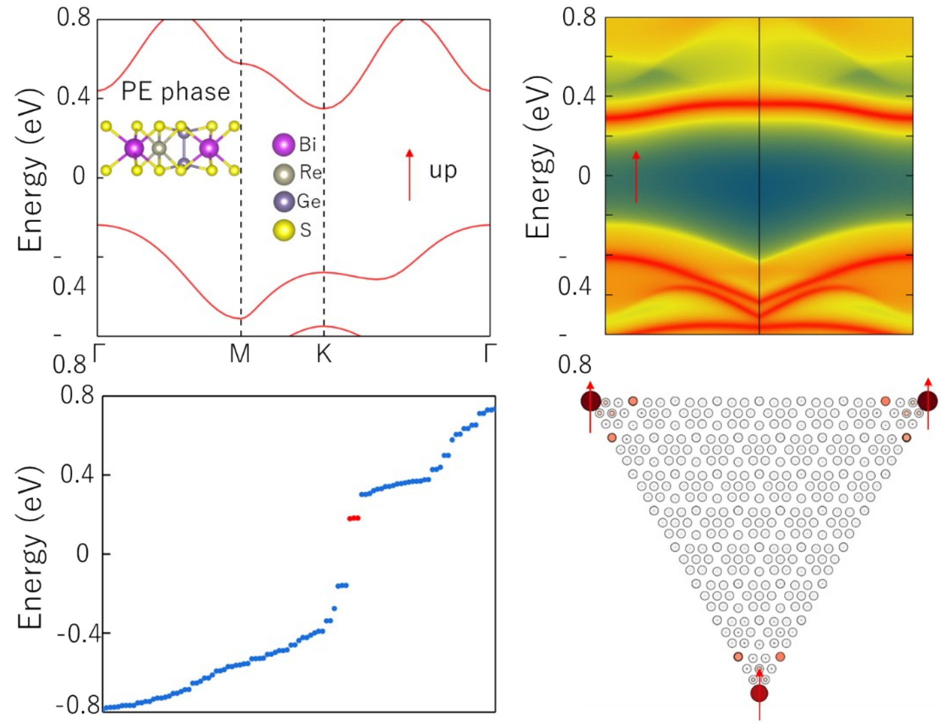

Fig. S 12 (a) Electronic band structures of PE phases in spin-up channel for $ReBiGe_2S_6$. (b) Projected spectrum in spin-up channel for $ReBiGe_2S_6$. (c) The corresponding energy levels in spin-down channel for $ReBiGe_2S_6$. (d) The charge distribution of the finite-sized nanodisks.

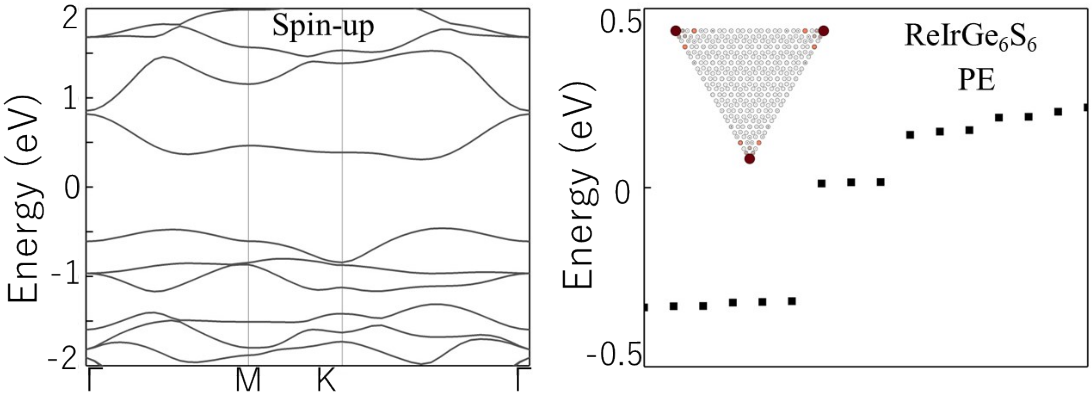

Fig. S 13 (a) Electronic band structures of PE phases in spin-up channel for $ReIrGe_2S_6$. (b)The corresponding energy levels in spin-up channel for $ReIrGe_2S_6$, and the charge distribution of the finite-sized nanodisks.

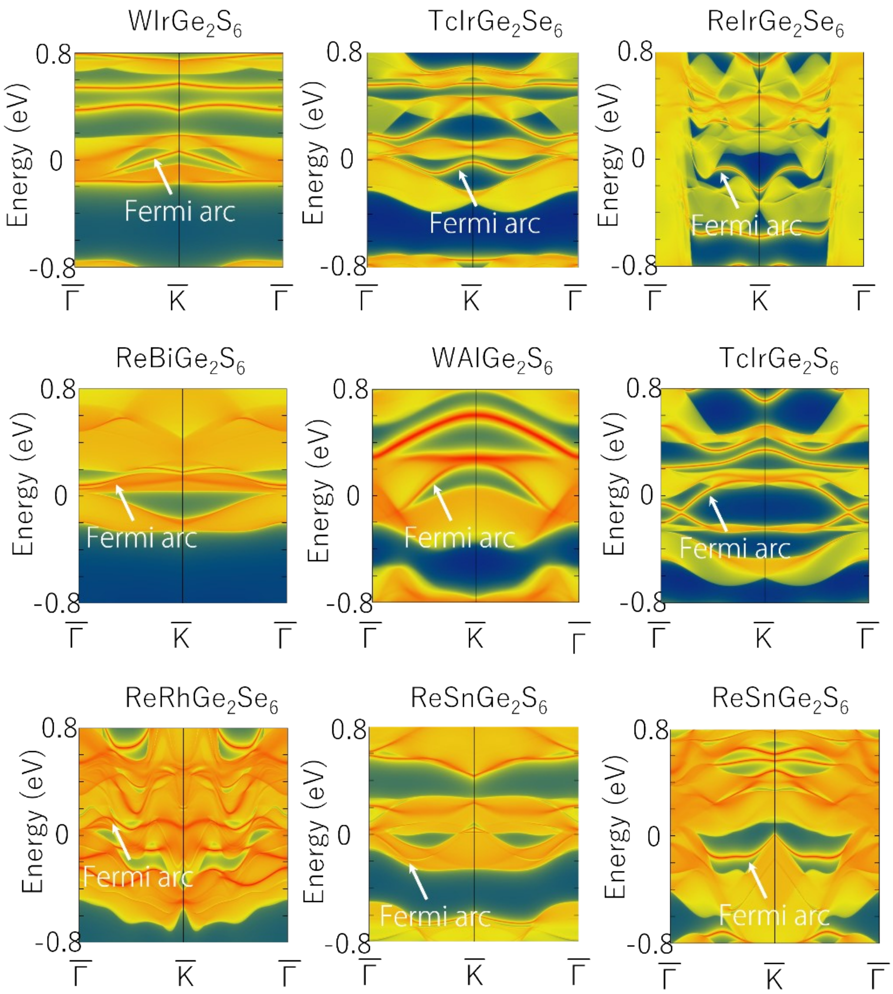

Fig. S 14. The band projections along the (100) direction for the $M_IM_{II}Ge_2X_6$ family with Weyl points. Among them, the last two band projections are the edge states of PE and FE phases for $ReSnGe_2S_6$.